

A Semi-Blind Watermarking Scheme for Color Images

Ersin Elbasi

The Graduate Center, CUNY
365 Fifth Avenue, New York, NY 10016, USA
eelbasi@gc.cuny.edu

Ahmet M. Eskicioglu

Department of CIS, Brooklyn College, CUNY
2900 Bedford Avenue, Brooklyn, NY 11210, USA
eskicioglu@sci.brooklyn.cuny.edu

Abstract—A DWT-based semi-blind image watermarking scheme leaves out the low pass band, and embeds the watermark in the other three bands into the coefficients that are higher than a given threshold T_1 . During watermark detection, all the high pass coefficients above another threshold T_2 ($T_2 > T_1$) are used in correlation with the original watermark [1]. In our extension to the DWT-based approach, we embed the same watermark in two bands (LL and HH) using different scaling factors for each band in the luminance layer of color image. In the watermark detection algorithm, the watermarked RGB (and possibly attacked) image is converted to the YUV model. After computing the DWT of the luminance layer, all the DWT coefficients higher than a given threshold T_2 in the LL and HH bands are selected. The next step is to compute the sum Z , where i runs over all DWT coefficients higher than a given threshold T_2 in the LL and HH bands. In each band, if Z exceeds T_z , the watermark is present. Experimental results indicate that detection in the LL band is robust for one group of attacks, and detection in the HH band is robust for another group of attacks.

Index Terms— semi-blind image watermarking, discrete wavelet transform, LL band, HH band, attacks.

I. INTRODUCTION

Content owners (e.g., movie studios and recording companies) have identified two major technologies for the protection of multimedia data: encryption and watermarking. A digital watermark is a pattern of bits inserted into a multimedia element such as a digital image, an audio or video file. In particular, watermarking appears to be useful in plugging the analog hole in consumer electronics devices. In applications such as owner identification, copy control, and device control, the most important properties of a watermarking system are robustness, invisibility, data capacity, and security [2].

In a classification of image watermarking schemes, several criteria can be used. Three of such criteria are the type of domain, the type of watermark, and the type of information needed in the detection or extraction process. According to the domain type, we have pixel domain and transform domain watermarking schemes. In the pixel domain, the pixel values are modified to embed the watermark. In the transform domain, the transform coefficients are modified to embed the watermark. Two-dimensional DWT can be implemented using

digital filters and downsamplers. Each level of decomposition produces four bands of data denoted by LL, HL, LH, and HH. The LL subband can further be decomposed to obtain another level of decomposition. This process is continued until the desired number of levels determined by the application is reached [3,4,5].

II. ALGORITHM

In a recent DCT-domain semi-blind image watermarking scheme, a pseudo-random number (PRN) sequence is embedded in a selected set of DCT coefficients [6]. The watermark is consisted of a sequence of real numbers $X = \{x_1, x_2, \dots, x_M\}$, where each value x_i is chosen independently according to $N(0,1)$. $N(\mu, \sigma^2)$ denotes a normal distribution with mean μ and variance σ^2 . In particular, after reordering all the DCT coefficients in a zig-zag scan, the watermark is embedded in the coefficients from the $(L+1)$ st to the $(M+L)$ th. The first L coefficients are skipped to achieve perceptual transparency.

A DWT-based semi-blind image watermarking scheme follows a similar approach. Instead of using a selected set of DWT coefficients, the authors leave out the low pass band, and embed the watermark in the other three bands into the coefficients that are higher than a given threshold T_1 . During watermark detection, all the high pass coefficients above another threshold T_2 ($T_2 \geq T_1$) are used in correlation with the original watermark [2]. We extended the idea, and embedded PRN watermark into both LL and HH bands. The proposed watermark embedding and detection algorithms can be summarized as follows:

Watermark embedding:

1. Convert the $N \times N$ RGB image to YUV.
2. Compute the DWT of the luminance layer.
3. Embed the same PRN sequence into the DWT coefficients higher than a given threshold T_1 in the LL and HH bands: $T = \{t_i\}$, $t'_i = t_i + \alpha |t_i| x_i$, where i runs over all DWT coefficients $> T_1$.
4. Replace $T = \{t_i\}$ with $T' = \{t'_i\}$ in the DWT domain.
5. Compute the inverse DWT to obtain the watermarked image P .

Watermark detection:

1. Convert the $N \times N$ watermarked (and possibly attacked) RGB image to YUV.
2. Compute the DWT of the luminance layer.
3. Select all the DWT coefficients higher than T_2 in LL and HH bands.
4. Compute the sum $z = \frac{1}{M} \sum_{i=1}^M y_i t_i^*$, where i runs over all DWT coefficients $> T_2$, y_i represents either the real watermark or a fake watermark, t_i^* represents the watermarked and possibly attacked DWT coefficients.
5. Choose a predefined threshold $T_z = \frac{\alpha}{2M} \sum_{i=1}^M |t_i^*|$.
6. In both band, if z exceeds T_z , the conclusion is that the watermark is present.

III. EXPERIMENTS

Several orthogonal wavelet filters such as the Haar filter or the Daubechies filters can be used to compute the DWT. In our experiments, we obtained the first level decomposition using the Haar filter [7,8,9]. The values of α and the threshold for each band are given in Table 1.

Table 1. Scaling factor α and threshold T

Parameters/Bands	LL	HH
α	0.4	3.5
T_1	15	45
T_2	25	55

The 512x512 original test image, the watermarked image, and their difference are shown in Figure 2.

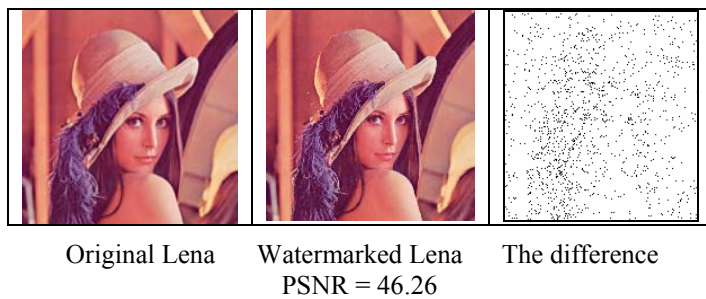


Figure 2. Embedding two watermarks into an image

Matlab was used for all attacks. The chosen attacks were JPEG compression, resizing, adding Gaussian noise, low pass filtering, rotation, histogram equalization, contrast adjustment, gamma correction, and cropping. In Figures 4-13, we display the detector responses for the real watermark, and 99 randomly generated watermarks. In each figure, the

correlation with the real watermark is located at 80 on the x -axis, and the dotted line shows the value of the threshold.



Figure 3. Attacks on watermarked Lena

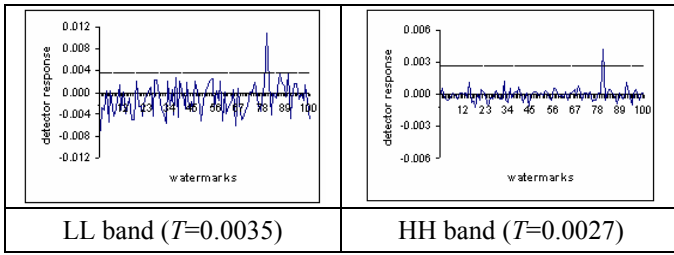


Figure 4. Detector response for unattacked watermarked Lena

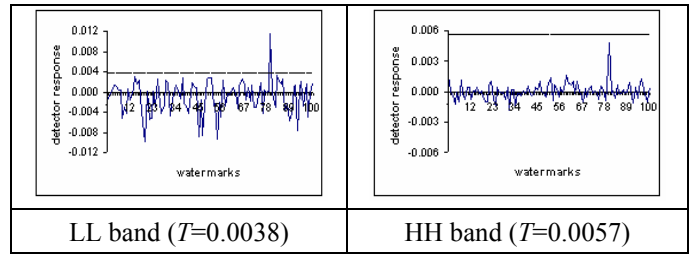


Figure 9. Detector response for low pass filtering

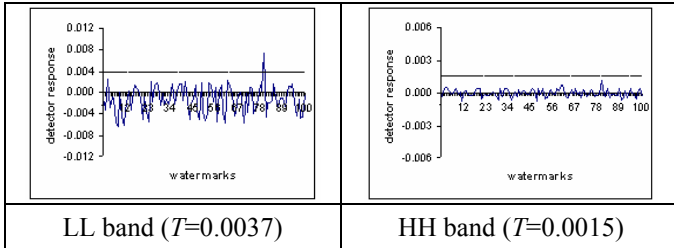


Figure 5. Detector response for JPEG compression: Q=25

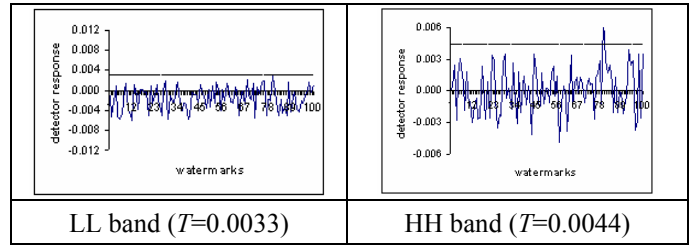


Figure 10. Detector response for histogram equalization

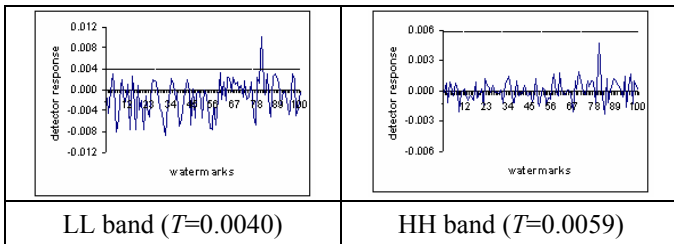


Figure 6. Detector response for Gaussian noise

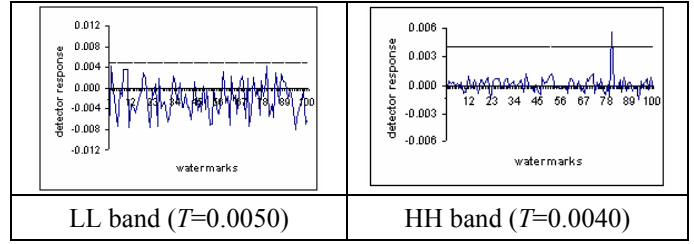


Figure 11. Detector response for contract adjustment

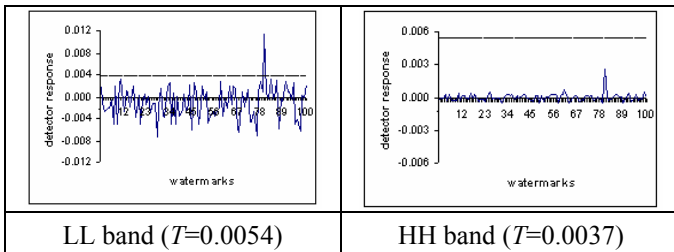


Figure 7. Detector response for resizing

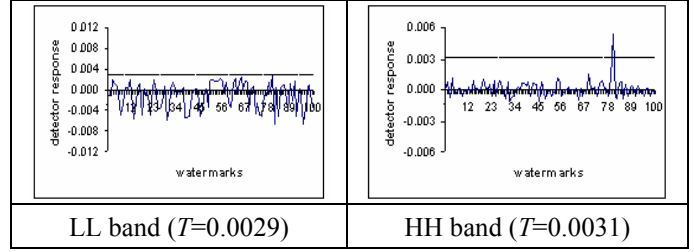


Figure 12. Detector response for gamma correction

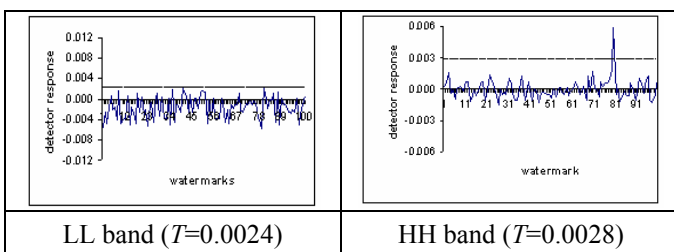


Figure 8. Detector response for cropping

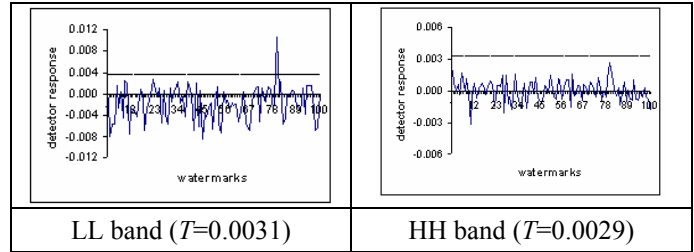


Figure 13. Detector response for rotation (5°)

IV. CONCLUSIONS

In a DWT-based semi-blind image watermarking paper, a watermark is embedded in three bands, leaving out the low pass subband, using coefficients that are higher than a given threshold T_1 . During watermark detection, all the high pass coefficients higher than another threshold T_2 ($T_2 \geq T_1$) are chosen for correlation with the original watermark.

In this paper, we have extended the idea by embedding the same watermark in two bands (LL and HH) using different scaling factors and thresholds for each band in color images.

Our experimental results show that for one group of attacks (JPEG compression, resizing, adding Gaussian noise, low pass filtering, and rotation), the correlation with the real watermark is higher than the threshold in the LL band, and for another group of attacks (histogram equalization, contrast adjustment, gamma correction, and cropping), the correlation with the real watermark is higher than the threshold in the HH band.

V. REFERENCES

- [1] R. Dugad, K. Ratakonda, and N. Ahuja, "A New Wavelet-Based Scheme for Watermarking Images," *Proceedings of 1998 International Conference on Image Processing (ICIP 1998)*, Vol. 2, Chicago, IL, October 4-7, 1998, pp. 419-423.
- [2] E. Elbasi and A. M. Eskicioglu, "A DWT-based Robust Semi-blind Image Watermarking Algorithm Using Two Bands," IS&T/SPIE's 18th Symposium on Electronic Imaging, Security, Steganography, and Watermarking of Multimedia Contents VIII Conference, San Jose, CA, January 15-19, 2006.
- [3] C.-H. Lee and Y.-K. Lee, "An Adaptive Digital Image Watermarking Technique for Copyright Protection," *IEEE Transactions on Consumer Electronics*, 45(4), November 1999, pp. 1005-1015.
- [4] I. J. Cox, J. Kilian, T. Leighton and T. Shamoon, "Secure Spread Spectrum Watermarking for Multimedia," *IEEE Transactions on Image Processing*, 6(12), December 1997, pp. 1673-1687.
- [5] W. Zhu, Z. Xiong and Y.-Q. Zhang, "Multiresolution Watermarking for Images and Video," *IEEE Transactions on Circuits and Systems for Video Technology*, 9(4), June 1999, pp. 545-550.
- [6] A. Piva, M. Barni, F. Bartolini, V. Cappellini, "DCT-based Watermark Recovering without Resorting to the Uncorrupted Original Image," *Proceedings of the 1997 International Conference on Image Processing (ICIP '97)*, Washington, DC, USA, October 26-29, 1997.
- [7] V. Licks and R. Jordan, "On Digital Image Watermarking Robust to Geometric Transformations," *Proceedings of 2000 International Conference Image Processing (ICIP 2000)*, Vol. 3, Vancouver, BC, Canada, September 10-13, 2000, pp. 690-693.
- [8] C.-Y. Lin, M. Wu, J. A. Bloom, I. J. Cox, M. L. Miller, and Y. M. Lui, "Rotation, Scale, and Translation Resilient Watermarking for Images," *IEEE Transactions on Image Processing*, 10(5), May 2001, pp. 767-782.
- [9] R. Caldelli, M. Barni, F. Bartolini, A. Piva, "Geometric-Invariant Robust Watermarking through Constellation Matching in the Frequency Domain," *Proceedings of the 2000 International*